



H₂S interaction with Cu(100)-(2 × 2)_{R45°}-O: Formation of a metastable 05 52sulfur surface reconstruction

Colaianni, M. L.; Syhler, P.; Chorkendorff, Ib

Published in:
Physical Review B Condensed Matter

Link to article, DOI:
[10.1103/PhysRevB.52.2076](https://doi.org/10.1103/PhysRevB.52.2076)

Publication date:
1995

Document Version
Publisher's PDF, also known as Version of record

[Link back to DTU Orbit](#)

Citation (APA):
Colaianni, M. L., Syhler, P., & Chorkendorff, I. (1995). H₂S interaction with Cu(100)-(2 × 2)_{R45°}-O: Formation of a metastable 05 52sulfur surface reconstruction. *Physical Review B Condensed Matter*, 52(3), 2076-2082.
DOI: 10.1103/PhysRevB.52.2076

DTU Library

Technical Information Center of Denmark

General rights

Copyright and moral rights for the publications made accessible in the public portal are retained by the authors and/or other copyright owners and it is a condition of accessing publications that users recognise and abide by the legal requirements associated with these rights.

- Users may download and print one copy of any publication from the public portal for the purpose of private study or research.
- You may not further distribute the material or use it for any profit-making activity or commercial gain
- You may freely distribute the URL identifying the publication in the public portal

If you believe that this document breaches copyright please contact us providing details, and we will remove access to the work immediately and investigate your claim.

H₂S interaction with Cu(100)-(2√2×√2)R 45°-O: Formation of a metastable $\begin{smallmatrix} 5 & 2 \\ 0 & 5 \end{smallmatrix}$ -sulfur surface reconstruction

M. L. Colaianni,* P. Syhler, and I. Chorkendorff†

Physics Department, Building 307, Technical University of Denmark, DK-2800 Lyngby, Denmark

(Received 23 January 1995)

This paper utilizes scanning tunneling microscopy, low-energy electron diffraction, Auger-electron spectroscopy, and temperature-programmed desorption to examine a metastable $\begin{smallmatrix} 5 & 2 \\ 0 & 5 \end{smallmatrix}$ -S structure which forms after the interface reaction of H₂S with a Cu(100)-(2√2×√2)R 45°-O surface. This preoxidized copper surface displays an enhanced reactivity towards H₂S compared to the clean and annealed Cu(100) surface. Exposing 15 L of H₂S onto a Cu(100)-(2√2×√2)R 45°-O surface causes all the adsorbed oxygen to desorb as H₂O at 164 K, while leaving approximately 0.5 ML of adsorbed sulfur on the surface. When this sulfur overlayer is annealed between 525 and 600 K, a metastable $\begin{smallmatrix} 5 & 2 \\ 0 & 5 \end{smallmatrix}$ -S reconstruction forms that is not observed after annealing similar coverages of sulfur adsorbed on an initially clean Cu(100) surface. Heating the $\begin{smallmatrix} 5 & 2 \\ 0 & 5 \end{smallmatrix}$ -S surface to temperatures above 600 K converts this structure to the thermally stable Cu(100)-(√17×√17)R 14°-S (i.e., $\begin{smallmatrix} 4 & 1 \\ 1 & 4 \end{smallmatrix}$ -S overlayer). A model for the metastable $\begin{smallmatrix} 5 & 2 \\ 0 & 5 \end{smallmatrix}$ -S reconstruction is proposed.

I. INTRODUCTION

An advantage of the scanning tunneling microscope is its ability to examine surface structures with large unit cells, which, due to their complexity, cannot be easily studied by traditional surface-sensitive structural tools. Scanning tunneling microscopy (STM) derives its advantage from its ability to directly image unit cells individually, and in real space, thus negating the complications that arise in diffraction techniques when they are used to measure structures composed of many atoms and/or several domains.

To date, most studies of H₂S on preoxidized surfaces have concentrated on the chemistry of the interface. In these studies, H₂S reaction with preoxidized surfaces is shown to form water while leaving sulfur on the metal surface. Processes of this nature have been reported on Pt(111),¹ Ni(110),² Ni(100),³ Cu(110),^{4,5} Cu(111),⁶ and on Pb films.⁷ Recently though, the structural aspects of this interface reaction have been examined. Real time studies of H₂S exposed onto a preoxidized Ni(110) surface using STM [Ref. 8(a)] revealed that by dosing H₂S onto a preoxidized surface, a $p(4\times 1)$ -S reconstructed layer could be obtained at room temperature, whereas such a structure only formed on the H₂S-dosed clean Ni(110) upon annealing to ≥ 473 K.⁹ The reason proposed for this low-temperature formation of the $p(4\times 1)$ was that a H₂S reaction with the O-reconstructed surface produces a rougher surface layer which possesses a higher surface energy than the initially flat metal surface. Such a higher-energy surface facilitates the formation of the $p(4\times 1)$ structure by reducing the energy barrier for its production.⁸ Very recently similar investigations have been undertaken for the H₂S interaction with preoxidized Cu(110).^{8(b)} The surface is, in effect, preactivated by the oxygen.

This paper studies the chemistry and the structure that result from the reaction of H₂S on Cu(100)-(2√2×√2)R 45°-O. We utilize STM, in addition to Auger-electron spectroscopy (AES), low-energy electron diffraction (LEED), and temperature-programmed desorption (TPD) to probe the reaction at this interface, and to examine a metastable sulfur reconstruction on the Cu(100) surface. This sulfur reconstruction, produced only upon annealing a H₂S-exposed preconstructed Cu(100)-(2√2×√2)R 45°-O layer, has a unit cell structure $\begin{smallmatrix} 5 & 2 \\ 0 & 5 \end{smallmatrix}$, for which we propose a structural model containing a sulfur coverage of 0.48 ML. The well-formed $\begin{smallmatrix} 5 & 2 \\ 0 & 5 \end{smallmatrix}$ -S was found to be formed upon annealing a sulfur coverage of ~ 0.5 ML adsorbed on the Cu(100)-(2√2×√2)R 45°-O surface in the temperature range 525–600 K. Above 600 K, the $\begin{smallmatrix} 5 & 2 \\ 0 & 5 \end{smallmatrix}$ -S irreversibly converts to the $\begin{smallmatrix} 4 & 1 \\ 1 & 4 \end{smallmatrix}$ -S structure,^{10–13} which is thermally stable to temperature of at least 1273 K. We propose that the route to the $\begin{smallmatrix} 5 & 2 \\ 0 & 5 \end{smallmatrix}$ -S structure is enabled by the preconstruction of the terraces by the adsorbed oxygen of the Cu(100)-(2√2×√2)R 45°-O surface.

II. EXPERIMENT

The experiments reported in this manuscript were performed in a stainless-steel ultrahigh vacuum (UHV) chamber that has been described in detail previously.¹⁰ Briefly, the chamber houses a single-pass Perkin-Elmer Auger-electron spectrometer, a copper-shielded Balzers QMG 421 C quadrupole mass spectrometer, and a Princeton Research Instruments model 8-120 reverse view LEED apparatus. The principal component in the chamber was a Danish Micro Engineering model 3000 UHV scanning tunneling microscope which we modified to accommodate our custom-designed Cu(100) crystal holder. The scanning tunneling microscope was operated

with 0.5-mm W wire, which was electropolished to a sharp point using the drop-off tip-preparation method.^{14,15}

H₂S (Linde, 98% purity) was subjected to two freeze-pump-thaw cycles prior to use. O₂ (Alfax, 99.9995% purity) was used without further purification. The purity of these gases was verified using a quadrupole mass spectrometer prior to their use. The Cu(100) crystals used in these studies were spark cut, mechanically polished to a mirrorlike surface, and then electropolished in an ~60% phosphoric acid at 2 V for 1–2 min. This final step usually lifted the mirrorlike surface, but LEED and STM analysis confirmed well-ordered surfaces after sputtering and annealing.

III. RESULTS

A. H₂S reactivity with the Cu(100)-(2√2×√2)R45°-O surface

Figure 1 compares Auger uptake curves of H₂S exposures onto a clean Cu(100) surface and a Cu(100)-(2√2×√2)R45°-O surface at 300 K. As is readily apparent, H₂S reactivity is enhanced on the preoxidized copper surface relative to the clean copper surface. The initial uptake rate of sulfur is increased on the preoxidized surface, and lower H₂S exposures are necessary to achieve a surface-saturated sulfur layer. On the Cu(100)-(2√2×√2)R45°-O surface, H₂S exposures of only 30 L produce a S(152 eV)/Cu(60 eV) ratio close to saturation, ~1.0, whereas an ~10 000 L exposure of H₂S on clean Cu(100) is required to achieve a similar S coverage. Furthermore, exposing a Cu(100)-(2√2×√2)R45°-O surface to 12 L H₂S at room temperature causes a complete replacement of the oxygen on the surface by adsorbed sulfur (Fig. 1).

The sulfur coverage after equivalent exposures onto the clean and Cu(100)-(2√2×√2)R45°-O surface can be in-

vestigated by LEED and AES analysis. On the clean surface, a well-ordered $p(2\times 2)$ surface with only a minimal amount of streaks between the spots¹⁶ is obtained upon H₂S exposures of 8–12 L followed by a 573-K anneal, suggesting that a S/Cu ratio of 0.45 corresponds to a coverage of ~0.25 ML. Using this approximation, we determine that a 30-L H₂S dose onto the Cu(100)-(2√2×√2)R45°-O surface produces a surface coverage of ~0.5 ML, while a 30-L H₂S dose on a clean and annealed Cu(100) surface yields a S coverage of only ~0.3 ML.

The process whereby the surface oxygen is removed from the Cu(100)-(2√2×√2)R45°-O surface and replaced by adsorbed sulfur after dosing with H₂S can be studied by TPD as shown in Fig. 2. For this experiment, a Cu(100)-(2√2×√2)R45°-O layer is prepared and then cooled to ~100 K prior to a 15-L H₂S exposure. Upon heating of this interface, the only desorbing species detected was H₂O at 164 K. H₂ and H₂S were not observed from H₂S/O/Cu(100) interfaces when the H₂S exposures were ≤ 15 L suggesting that at these exposures all the hydrogen from the adsorbed H₂S molecules reacts with the adsorbed oxygen to produce water (Fig. 2).

B. Structure of the sulfided Cu(100)-(2√2×√2)R45°-O interface

1. LEED results

Figure 3(a) shows the (2√2×√2)R45°-O LEED pattern after oxidizing Cu(100) with 8000 L O₂ at 500 K. This structure has been studied extensively by LEED,^{17–19} photoelectron diffraction and near-edge x-ray absorption fine structure,²⁰ x-ray-diffraction,²¹ and STM.^{22–25} All have concluded that a reconstructed missing-row model, possessing an O coverage of 0.5 ML, best describes this surface. In this model, every fourth

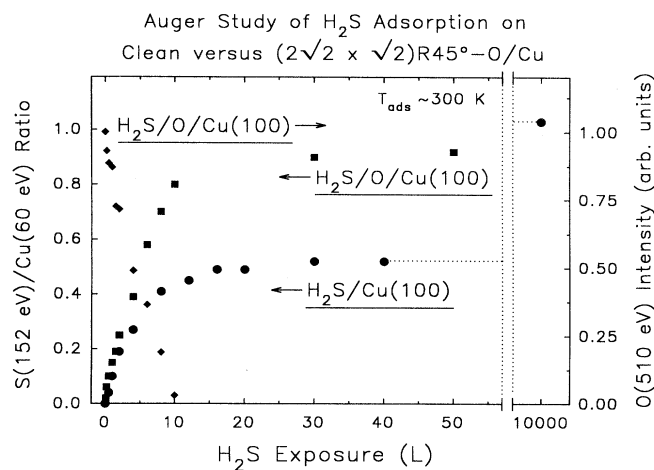


FIG. 1. Sulfur uptake curves comparing the reactivity of H₂S on clean and annealed Cu(100) vs a Cu(100)-(2√2×√2)R45°-O surface. Also provided is the oxygen attenuation from the Cu(100)-(2√2×√2)R45°-O layer as a function of H₂S exposure. All adsorbed oxygen is removed by H₂S exposures of > 10 L.

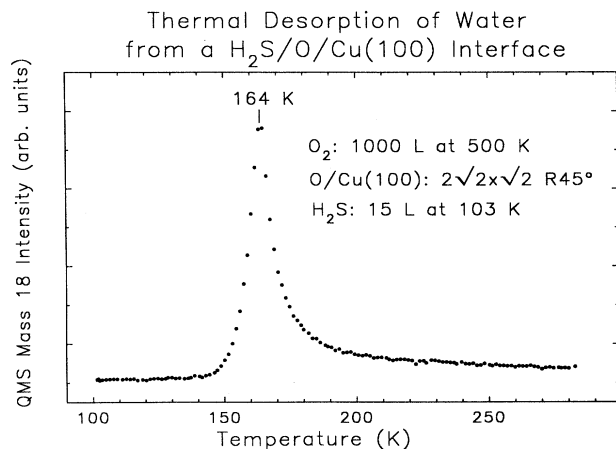


FIG. 2. A temperature-programmed desorption spectrum showing the desorption of water from a H₂S/Cu(100)-(2√2×√2)R45°-O interface. The heating rate was 1.0 K/s. The other masses monitored in this experiment were 2 (H₂), 32 (O₂), 34 (H₂S), 48 (SO), and 64 (SO₂) amu. Only mass 18 was detected.

row of copper atoms is ejected from the [001] direction into overlayer island structures, while Cu-O chains, also in the [001] direction, form in the terraces and on the newly formed islands.²³ The removal of $\frac{1}{4}$ of the Cu(100) terrace atoms can be explained to result from adsorbed oxygen overcoordinating electron density to surface copper atoms which causes these atoms to compensate by

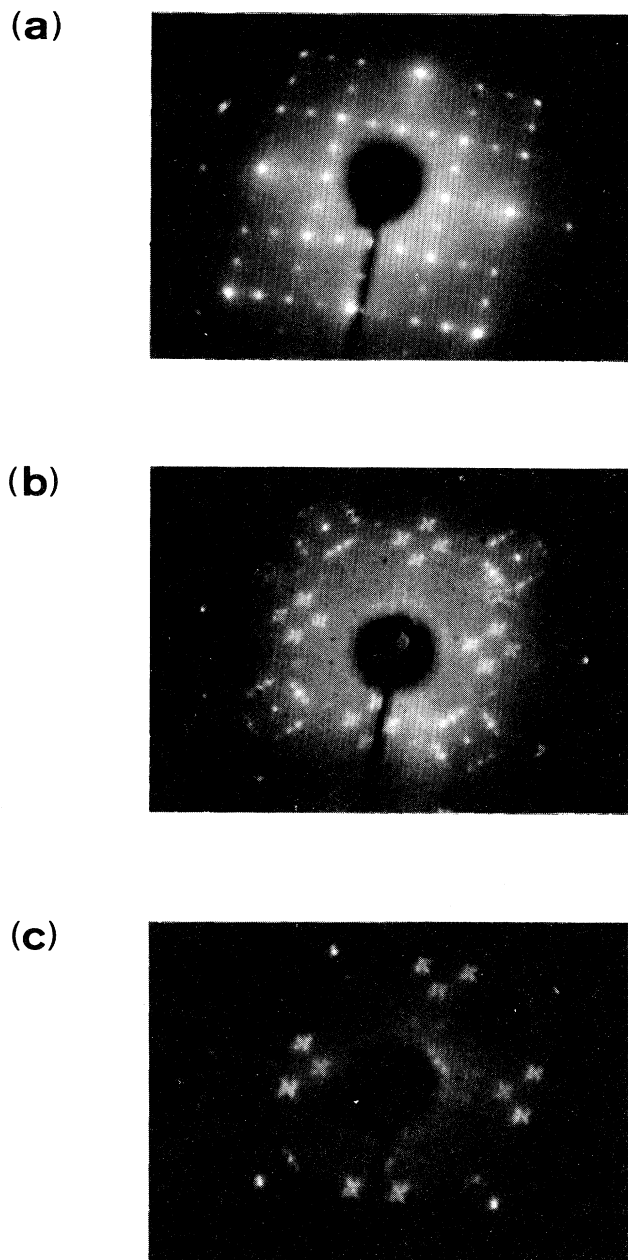


FIG. 3. LEED patterns showing O- and S-induced reconstructions of Cu(100): (a) A Cu(100)-(2 $\sqrt{2}$ \times $\sqrt{2}$)R45°-O surface prepared by exposing a clean and annealed Cu(100) to 8000 L O₂ at 500 K, $E_p = 194$ eV; (b) the $|\frac{5}{0} \frac{2}{3}|$ -S structure formed by dosing 100 L H₂S on a Cu(100)-(2 $\sqrt{2}$ \times $\sqrt{2}$)R45°-O surface at 309 K followed by annealing to 573 K, $E_p = 78.6$ eV, (c) same as (b) except H₂S = 10 L at 105 K, $E_p = 50.2$ eV.

reducing their coordination number by moving from *within* the surface to *on top* of the surface.²⁶ Copper atoms are stabilized in this overlayer arrangement by the stronger Cu-O bonds, which form on this reconstructed copper overlayer, compared to the unreconstructed layer.²⁷

Exposing this Cu(100)-(2 $\sqrt{2}$ \times $\sqrt{2}$)R45°-O layer to ≥ 10 L H₂S completely removes the ordered LEED pattern, leaving only faint and broad (1 \times 1) spots. However, upon annealing to 575 K, a previously unreported LEED pattern is observed, which is shown in Figs. 3(b) and 3(c). We identify this pattern as resulting from a $|\frac{5}{0} \frac{2}{3}|$ -S surface structure. This surface forms only upon annealing between 525 and 600 K; a sharp LEED pattern is not obtained at temperatures below 525 K, and above 600 K the 600 K the structure begins to convert to the ($\sqrt{17}$ \times $\sqrt{17}$)R14°-S/Cu(100) (i.e., $|\frac{4}{1} \frac{1}{4}|$ -S structure), which becomes well ordered by further annealing to 675 K. An expanded view of the $|\frac{5}{0} \frac{2}{3}|$ -S LEED structure is shown in Fig. 3(c).

2. STM results

STM analysis of the $|\frac{5}{0} \frac{2}{3}|$ -S structure shows that the surface consists of two domains of zigzagging segments of unit cells [Figs. 4(a) and 4(b)]. When viewed more closely [Fig. 4(c)], these unit cells are observed to contain six clearly resolved protrusions. These protrusions are structurally similar to those observed by us in a previous study of the $|\frac{4}{1} \frac{1}{4}|$ -S structure on Cu(100).¹⁰ To the best of our ability to measure the interatomic distances, we find the same spacing between neighboring protrusions on the $|\frac{5}{0} \frac{2}{3}|$ -S surface as was measured on the $|\frac{4}{1} \frac{1}{4}|$ -S surface, specifically, 4.0 ± 0.15 Å. The only difference appears to be the two additional features per unit cell, thus forming heximer instead of tetramer units. The zigzag appearance is produced by $|\frac{5}{0} \frac{2}{3}|$ and $|\frac{5}{0} \frac{2}{3}|$ unit cells within each of the domains.

IV. DISCUSSION

A. Chemistry of H₂S adsorption on Cu(100)-(2 $\sqrt{2}$ \times $\sqrt{2}$)R45°-O

1. Enhanced sulfur uptake

The sulfidation of Cu(100) is shown in Fig. 1 to be enhanced by preoxidizing the surface. By monitoring the ratio of the Auger S(152 eV)/Cu(60 eV) peak-to-peak heights as a function of H₂S exposure, we measure that the initial S uptake is increased by as much as a factor of 2 for exposures below 1 L H₂S. Also, H₂S exposures required to reach saturation differ by approximately two orders of magnitude. Sulfur saturation is achieved by ≤ 100 L H₂S on Cu(100)-(2 $\sqrt{2}$ \times $\sqrt{2}$)R45°-O, while H₂S exposures of ~ 10000 L are needed on the clean and annealed Cu(100) surface. In both cases, H blocking of sites for sulfur adsorption is not a factor since adsorbed H desorbs as H₂ on clean Cu(100) by 300 K,²⁸ and as H₂O on the preoxidized Cu(100) surface at 164 K.

Auger-electron spectroscopic analysis and thermal

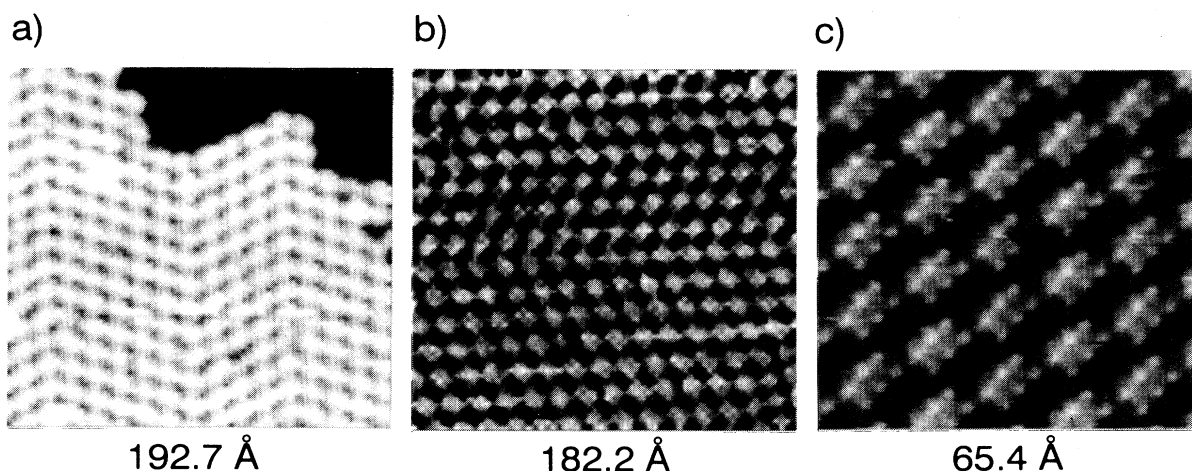


FIG. 4. STM images of the $|5 \ 2|_0 \ 5|$ -S surface prepared by dosing 100 L H₂S onto Cu(100)-(2√2×√2)R45°-O at 315 K followed by annealing to 573 K. All scans were performed with the sample at room temperature. Scan areas, sample bias, and tunneling currents were as follows: (a) 193×193 Å, $V_b=0.65$ V, $I_t=1.26$ nA, (b) 182×182 Å, $V_b=0.30$ V, $I_t=1.06$ nA, (c) 65×65 Å, $V_b=0.64$ V, $I_t=1.26$ nA.

desorption results reveal that the $|5 \ 2|_0 \ 5|$ -S layer possesses a sulfur coverage approximately equal to the coverage of O in the Cu(100)-(2√2×√2)R45°-O surface. The absence of an H₂ desorption peak (spectra not shown), as well as the total removal of adsorbed oxygen, as observed by AES, reveals that by dosing the Cu(100)-(2√2×√2)R45°-O surface with 15 L H₂S at 103 K (1) all the H₂S that is adsorbed loses its H to the surface oxygen, and (2) the amount of H₂S that adsorbs and reacts with the surface is equal to the oxygen coverage of the Cu(100)-(2√2×√2)R45°-O surface [$\Theta_O=0.48\pm0.05$ ML (Ref. 29)]. A similar observation was made by Huntley upon exposing H₂S onto high coverages of oxygen on Ni(110).² This confirms that the S coverage that forms the $|5 \ 2|_0 \ 5|$ -S structure is similar to that which forms the $|4 \ 1|_1 \ 4|$ -S structure ($\Theta_S=0.47$ ML).¹¹

Similar to our previous study of the (√17×√17)R14°-S surface,¹⁰ we find that variations of the sulfur coverage within a range of ~10% (as judged by AES) did not seem to greatly affect the quality of the $|5 \ 2|_0 \ 5|$ LEED pattern, but did affect the annealing temperature required to form the ordered sulfur structure. The $|5 \ 2|_0 \ 5|$ -S structure was observed after flash annealing the H₂S/Cu(100)-(2√2×√2)R45°-O interface to only 523 K on surfaces possessing initially high S coverages, while 573 K annealing was necessary to form the structure on surfaces with an initial lower S coverage.

This enhanced reactivity of H₂S by preoxidation of the surface is believed to result from the restructured state of the Cu(100) surface atoms within the Cu(100)-(2√2×√2)R45°-O structure. In our previous study of H₂S/Cu(100),¹⁰ STM images recorded during H₂S exposure revealed that sulfur coverages above ~0.25 ML adsorb on the Cu(100) surface via a terrace-restructuring mechanism, where copper atoms were removed from terrace sites while a disordered Cu-S overlayer formed. This mechanism allows a sulfur coverage of ~0.5 ML which, after annealing to 900 K, produces an ordered

(√17×√17)R14°-S structure.¹⁰ We propose that the enhanced rate of sulfur uptake on the Cu(100)-(2√2×√2)R45°-O surface results from the preresult of the copper atoms from terrace sites by adsorbed oxygen. This reduces the energy cost of accommodating increased sulfur coverages by eliminating the work required to restructure the Cu(100) surface. The energy difference between copper in its clean unreconstructed Cu(100) surface structure and in the reconstructed structure of the (2√2×√2)R45°-O surface has been calculated to be 0.30 eV.^{25,30}

2. Water formation upon H₂S adsorption on Cu(100)-(2√2×√2)R45°-O

Figure 2 shows that annealing a H₂S-dosed (2√2×√2)R45°-O/Cu(100) layer at 103 K with 15 L H₂S produces a H₂O desorption feature at 164 K. This corresponds closely to the 165-K desorption feature measured by Bange *et al.*³¹ for the onset of multilayer ice formation on Cu(110). In their study, monolayer coverages of water were measured to desorb between 167 and 174 K, while an -OH+-OH disproportionation reaction occurred at 290 K.³¹ Similar H₂O desorption temperatures resulting from molecular desorption and disproportionation reactions have been reported for a large variety of metal surfaces.³² The low desorption temperature observed in our studies suggests a weak interaction between the H₂O(a) and the sulfided surface.

Using solely TPD analysis, we cannot determine the mechanism by which, or the temperature at which, the H₂O forms on the surface since H₂O desorbs at the molecular desorption temperature. Remaining unresolved is whether H₂O forms immediately upon H₂S dosing at 103 K, or whether it forms in steps at temperatures above 103 K. Previous studies by Prabharan, Sen, and Rao⁴ using high-resolution electron energy loss spectroscopy have shown that H₂S/O/Cu(110) interfaces

do not show a -OH vibrational feature at 80 K, although an -OH feature is observed upon warming to 120 K. Moroney, Rassias, and Roberts⁶ used x-ray photoemission spectroscopy to show that on an H₂S exposed O/Cu(111) surface, both -OH and H₂-O features are observed at 105 K, but by 136 K H₂O is the major component with -OH existing as a minority species. This adsorbed H₂O desorbs by 173 K. These papers reveal a pattern of H₂O forming in steps as the H₂S dissociates above 80 K on the preoxidized copper surfaces. Verification of the exact mechanism on the preoxidized Cu(100) surface, though, awaits further study. However, we can conclude on the basis of the H₂O desorption temperature and the absence of any oxygen remaining on the surface at 165 K that H₂O formation on this interface does not occur via an -OH disproportionation reaction.

B. Surface structure after H₂S reaction with Cu(100)-(2√2×√2)R45°-O

Results from LEED, AES, and TPD show clearly that H₂S adsorption on the Cu(100)-(2√2×√2)R45°-O surface at 300 K results in a disordered overlayer composed solely of S and Cu. Similarly, disordering of the clean Cu(100) surface (1×1) structure was observed by STM and LEED after large exposures (>10 000 L) of H₂S. Evidence for mass transport of the surface metal atoms was provided by STM, which observed flat (100) terraces transform into crevasses and islands supporting chainlike structures. In similar studies, STM analysis during H₂S reaction with the O/Cu(100) surface has also shown mass transport of Cu on the surface resulting in the formation of large island structures.^{8(b)} In this study, however, a STM analysis of the disordering process on the Cu(100)-(2√2×√2)R45°-O interface was not performed. The removal of the LEED pattern upon H₂S adsorption though reveals that a disordering process also occurs at the oxidized interface. While the mechanistic details of this disordering are not known, a model involving Cu mass transport as observed on the clean Cu(100) surface¹⁰ and the preoxidized Cu(110) surface^{8(b)} is believed to be occurring.

Upon warming to 373 K, the LEED pattern shows large broad spots where the four-point features appear on the LEED pattern of the well-formed $\begin{smallmatrix} 5 & 2 \\ 0 & 5 \end{smallmatrix}$ -S surface. Similar broad features were always observed after annealing larger doses (10 000 L) of H₂S onto the clean Cu(100) surface. Careful annealing of this H₂S/Cu(100) interface produced only these broad spots until the $\begin{smallmatrix} 4 & 1 \\ 1 & 4 \end{smallmatrix}$ -S formed at ~973 K.¹⁰ In addition, experiments which used a line-of-sight heated filament during H₂S dosing to deposit sulfur coverages ≥ 0.5 ML also failed to yield the $\begin{smallmatrix} 5 & 2 \\ 0 & 5 \end{smallmatrix}$ -S structure after annealing, despite the necessary quantity of adsorbed sulfur on the surface. Only by sulfiding a Cu(100)-(2√2×√2)R45°-O layer could the well-ordered $\begin{smallmatrix} 5 & 2 \\ 0 & 5 \end{smallmatrix}$ -S structure be formed prior to the $\begin{smallmatrix} 4 & 1 \\ 1 & 4 \end{smallmatrix}$ -S.

These observations lead us to propose that the ordered metastable $\begin{smallmatrix} 5 & 2 \\ 0 & 5 \end{smallmatrix}$ -S structure must involve a large kinetic barrier to formation on the clean Cu(100) surface, requiring temperatures beyond those which cause the onset of

the thermodynamically stable $\begin{smallmatrix} 4 & 1 \\ 1 & 4 \end{smallmatrix}$ -S structure. Therefore, the ordered $\begin{smallmatrix} 5 & 2 \\ 0 & 5 \end{smallmatrix}$ -S overlayer is not observed from the clean surface. However, beginning with a reconstructed Cu(100)-(2√2×√2)R45°-O surface, the barrier to formation of the $\begin{smallmatrix} 5 & 2 \\ 0 & 5 \end{smallmatrix}$ -S is lowered to become accessible at 525 K. This is believed to result from the O-induced restructuring of the copper atoms from the flat (100) surface to the higher-energy Cu(100)-(2√2×√2)R45°-O structure.²⁷ From this higher-energy starting point, the barrier to formation of the $\begin{smallmatrix} 5 & 2 \\ 0 & 5 \end{smallmatrix}$ -S is lower and becomes accessible prior to the onset of the $\begin{smallmatrix} 4 & 1 \\ 1 & 4 \end{smallmatrix}$ -S.

The most obvious feature of the $\begin{smallmatrix} 5 & 2 \\ 0 & 5 \end{smallmatrix}$ -S is its herringlike structure. This results from alternating chains of $\begin{smallmatrix} 5 & 2 \\ 0 & 5 \end{smallmatrix}$ and $\begin{smallmatrix} 5 & 0 \\ 2 & 5 \end{smallmatrix}$ unit cells. These chains vary between 1 and 10 unit cells in length, with lengths between 4 and 6 unit cells being the most common. This preference suggests that a structural strain is inherent within the overlayer structure, since a strain-free layer should display either (1) one orientation only, if attractive interactions existed between the cells, or (2) purely random orderings of $\begin{smallmatrix} 5 & 2 \\ 0 & 5 \end{smallmatrix}$ and $\begin{smallmatrix} 5 & 0 \\ 2 & 5 \end{smallmatrix}$ unit cells, if attractive interactions did not exist between the unit cells. These purely random orderings would display a probability *P* of chains to form of given length *n* to follow the form $P = 2(\frac{1}{2})^n$, which would favor very short chain lengths.

Such a favoring of very short chain lengths or of the one-orientation domains is not observed. Instead, it appears that unit cells stabilize neighboring cells of the same orientation, and thus grow in finite lengths of one orientation, but that a strain associated with possessing solely one orientation on the copper substrate increases with increasing chain length—since very long chains are not favored. Thus the zigzag pattern reduces the strain within the $\begin{smallmatrix} 5 & 2 \\ 0 & 5 \end{smallmatrix}$ -S overlayer, but it apparently does not cause it to be as stable as the $\begin{smallmatrix} 4 & 1 \\ 1 & 4 \end{smallmatrix}$ -S, to which the $\begin{smallmatrix} 5 & 2 \\ 0 & 5 \end{smallmatrix}$ -S converts upon warming to 573 K. Therefore, the $\begin{smallmatrix} 5 & 2 \\ 0 & 5 \end{smallmatrix}$ -S is observed only as a metastable surface structure.

The $\begin{smallmatrix} 5 & 2 \\ 0 & 5 \end{smallmatrix}$ -S unit cell is shown by STM to be composed of six resolved protrusions. These protrusions are believed to result from adsorbed sulfur. This is based, in part, on the calculations performed by Lang,³³ who shows for tip biases below ~1.3 V that an adsorbed S adds to the density of states in this energy range, and therefore is imaged as a protrusion. In addition, numerous STM studies of S adsorption on a variety of metal surfaces have assigned the protrusions resolved in their images to sulfur. These surfaces include Cu(111),³⁴ Cu(110),³⁵ Cu(11,1,1),³⁶ Ni(111),²⁶ Ni(110),^{9,37} Re(0001),^{38,39} Pd(111),⁴⁰ Pd(100),⁴¹ and Mo(100).⁴² Finally, our own STM studies of the *p*(2×2)-S overlayer gave protrusion at interatomic 2*a*₀ distances.

Our model proposed for the $\begin{smallmatrix} 5 & 2 \\ 0 & 5 \end{smallmatrix}$ -S structure, shown in Fig. 5, contains 12 sulfur atoms, for a sulfur coverage of 0.48, in accord with our AES and TPD results. Since only six features per unit cell are imaged, the surface is postulated to contain two types of sulfur atoms. The six resolved sulfur atoms are assigned to pseudo-fourfold-hollow sites (FFHS) on the top copper layer. These sites are chosen since surface sulfur should readily be imaged by STM [as in the *p*(2×2) layer] and since sulfur favors

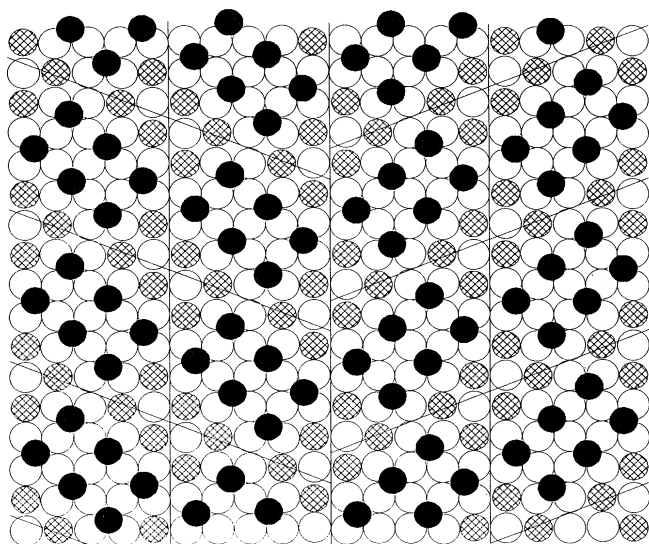


FIG. 5. Model of the $|0 \frac{5}{2}|$ -S structure. Black filled circles represent surface sulfur atoms in pseudo-FFHS, cross-hatched circles represent in-plane sulfur atoms which substitute for copper atoms in the surface layer, and the white circles represent copper atoms. The unit cells of one domain are shown. Equivalent $|0 \frac{5}{2}|$ and $|\frac{5}{2} \frac{0}{3}|$ unit cells are shown to produce the zig-zag pattern observed. See text for details.

sites of high coordination. Additionally, these are the sites on the copper surface that most closely allow for the measured sulfur interatomic separation of 4.0 ± 0.15 Å. While the unreconstructed $\sqrt{2}a_0$ sites are only 3.6 Å apart, distortions within the top layer are proposed to cause this increased S-S separation. This is consistent with the observed herring-row structure, which will release some of the stress built up by this expansion.

The regions of the surface which are imaged as depressions are proposed to contain the remaining six sulfur atoms of the unit cell. These sulfur atoms are proposed to occupy sites *within* the top copper layer, replacing copper atoms in the surface plane. These sulfur atoms will be referred to as in-plane sulfur atoms. While there is no direct evidence for the positions assigned to the in-plane sulfur atoms, such sites are reasonable for the following reasons: (1) high coverages of sulfur are known to reconstruct the top copper layer by removing copper atoms from terrace sites¹⁰—and these empty sites should be ideal for sulfur, which always bonds most favorably in sites of high coordination; (2) the interatomic repulsion

between adsorbed sulfur atoms will tend to drive the sulfur atoms as far apart as possible, which is only possible by placing sulfur atoms in the regions imaged as depressions; and (3) the S-Cu bond lengths in covellite, CuS [$d_{\text{CuS}} = 2.19\text{--}2.33$ Å] (Ref. 43) and other Cu-S compounds ($d_{\text{CuS}} = 2.16\text{--}2.33$ Å) (Ref. 44) are shorter than the bulk Cu-Cu bond length (2.55 Å). Therefore, these in-plane sulfur atoms would be expected to cause an inward repositioning of their neighboring copper atoms. These copper atoms make up the FFHS which adsorb the surface sulfur atoms. Consequently, this distorts the FFHS and allows the sulfur atoms in these FFHS to expand their interatomic distances, as the images indicate. This model is similar to one proposed by us in an earlier study of the $|\frac{4}{1} \frac{1}{4}|$ -S surface.¹⁰ Additional details of the S/Cu(100) interface are contained therein.

V. CONCLUSION

This paper centers around the discovery of a metastable sulfur structure with a unit cell $|0 \frac{5}{2}|$, which forms upon dosing H₂S onto a Cu(100)-(2√2×√2)R45°-O surface. This sulfur structure and the reaction that produces it have been characterized by the complementary techniques of LEED, STM, TPD, and AES. We arrive at the following conclusions: (1) Sulfur uptake from H₂S adsorption is enhanced on a Cu(100)-(2√2×√2)R45°-O surface compared to the clean and annealed Cu(100) surface. (2) H₂S dissociatively adsorbs on the Cu(100)-(2√2×√2)R45°-O surface, causing water formation and desorption by 164 K, and forming a disordered copper-sulfur overlayer. H₂S exposures between 10 and 100 L leave a sulfur coverage of ~0.5 ML. (3) Annealing this disordered copper-sulfur layer to temperatures between 525 and 600 K produces an ordered $|0 \frac{5}{2}|$ -S metastable surface. (4) Continued annealing to, or above, 600 K causes the $|0 \frac{5}{2}|$ -S structure to convert to a $|\frac{4}{1} \frac{1}{4}|$ -S overlayer. (5) A model for the $|0 \frac{5}{2}|$ structure consisting of 12 sulfur atoms per 25-atom Cu unit cell is proposed. This model proposes two types of adsorbed sulfur, six surface-sulfur atoms located in pseudo fourfold-hollow sites, and six in-plane sulfur atoms occupying Cu atom sites within the top copper layer.

ACKNOWLEDGMENT

We would like to gratefully acknowledge support for this work by the Danish Research Council through the "Center for Surface Reactivity."

*Present address: Exxon Research and Engineering Company, Corporate Research, Route 22 East, Annandale, NJ 08801.

†Author to whom correspondence should be addressed.

¹G. E. Mitchell, M. A. Schulz, and J. M. White, *Surf. Sci.* **197**, 379 (1988).

²D. R. Huntley, *Surf. Sci.* **240**, 24 (1990).

³Y. Zhou and J. M. White, *Surf. Sci.* **183**, 363 (1987).

⁴K. Prabharan, P. Sen, and C. N. R. Rao, *Surf. Sci.* **169**, L301 (1986).

⁵P. S. Uy, J. Bardolle, and M. Bujor, *Surf. Sci.* **134**, 713 (1983).

⁶L. Moroney, S. Rassis, and M. W. Roberts, *Surf. Sci.* **105**, L249 (1981).

⁷K. Kishi and M. W. Roberts, *J. Chem. Soc. Faraday Trans. I* **71**, 1721 (1975).

⁸(a) L. Ruan, F. Besenbacher, I. Stensgaard, and E. Laegsgaard, *Phys. Rev. Lett.* **69**, 3523 (1992); (b) F. Besenbacher, P. T. Sprunger, L. Ruan, L. Olesen, I. Stensgaard, and E. Laegsgaard, *Topics Catal.* **1**, 325 (1994).

- ⁹F. Besenbacher, I. Stensgaard, L. Ruan, J. K. Nørskov, and K. W. Jacobsen, *Surf. Sci.* **272**, 334 (1992).
- ¹⁰M. L. Colaianni and I. Chorkendorff, *Phys. Rev. B* **50**, 8798 (1994).
- ¹¹J. L. Domange and J. Oudar, *Surf. Sci.* **11**, 124 (1968).
- ¹²V. Maurice, J. J. Legendre, and M. Huber, *Surf. Sci.* **129**, 312 (1983).
- ¹³M. Huber and J. Oudar, *Surf. Sci.* **47**, 605 (1975).
- ¹⁴J. P. Song, N. H. Pryds, K. Glejbjøl, K. A. Mørch, A. R. Thölen, and L. N. Christensen, *Rev. Sci. Instrum.* **64**, 900 (1993).
- ¹⁵H. Lemke, T. Goddenhenrich, H. P. Bochem, U. Hartmann, and C. Heiden, *Rev. Sci. Instrum.* **61**, 2538 (1990).
- ¹⁶H. C. Zeng and K. A. R. Mitchell, *Can. J. Phys.* **65**, 500 (1987).
- ¹⁷H. C. Zeng, R. A. McFarlane, and K. A. R. Mitchell, *Surf. Sci.* **208**, L7 (1989).
- ¹⁸H. C. Zeng and K. A. R. Mitchell, *Surf. Sci.* **239**, L571 (1990).
- ¹⁹M. Sotito, *Surf. Sci.* **260**, 235 (1992).
- ²⁰M. C. Asensio, M. J. Ashwin, A. L. D. Kilcoyne, D. P. Woodruff, A. W. Robinson, Th. Lindner, J. S. Somers, D. E. Richen, and A. M. Bradshaw, *Surf. Sci.* **236**, 1 (1990).
- ²¹I. K. Robinson, E. Vlieg, and S. Ferrer, *Phys. Rev. B* **42**, 6954 (1990).
- ²²Ch. Wöll, R. J. Wilson, S. Chiang, H. C. Zeng, and K. A. R. Mitchell, *Phys. Rev. B* **42**, 11 926 (1990).
- ²³F. Jensen, F. Besenbacher, E. Laegsgaard, and I. Stensgaard, *Phys. Rev. B* **42**, 9206 (1990).
- ²⁴F. Besenbacher and I. Stensgaard, in *The Chemical Physics of Solid Surfaces and Heterogeneous Catalysis*, edited by D. A. King and D. P. Woodruff (Elsevier, New York, 1993), Vol. 7, Chap. 15.
- ²⁵F. Besenbacher and J. K. Nørskov, *Prog. Surf. Sci.* **44**, 5 (1993).
- ²⁶L. Ruan, I. Stensgaard, F. Besenbacher, and E. Laegsgaard, *Phys. Rev. Lett.* **71**, 2963 (1993).
- ²⁷K. W. Jacobsen and J. K. Nørskov, *Phys. Rev. Lett.* **65**, 1788 (1990).
- ²⁸I. Chorkendorff and P. B. Rasmussen, *Surf. Sci.* **248**, 35 (1991).
- ²⁹M. Wuttig, R. Franchy, and H. Ibach, *Surf. Sci.* **213**, 103 (1989).
- ³⁰J. K. Nørskov, *Rep. Prog. Phys.* **53**, 1253 (1990).
- ³¹K. Bange, D. E. Grider, T. E. Madey, and J. K. Sass, *Surf. Sci.* **136**, 38 (1984).
- ³²P. A. Thiel and T. E. Madey, *Surf. Sci. Rep.* **7**, 211 (1987).
- ³³N. D. Lang, *Phys. Rev. Lett.* **58**, 45 (1987).
- ³⁴L. Ruan, I. Stensgaard, F. Besenbacher, and E. Laegsgaard, *Ultramicroscopy* **42-44**, 498 (1992).
- ³⁵I. Stensgaard, L. Ruan, F. Besenbacher, F. Jensen, and E. Laegsgaard, *Surf. Sci.* **269/270**, 81 (1992).
- ³⁶S. Rousset, S. Gauthier, O. Siboulet, W. Sacks, M. Belin, and J. Klein, *Phys. Rev. Lett.* **63**, 1265 (1989).
- ³⁷L. Ruan, I. Stensgaard, E. Laegsgaard, and F. Besenbacher, *Surf. Sci.* **296**, 275 (1993).
- ³⁸D. F. Ogletree, C. Ocal, B. Marchon, G. A. Somorjai, M. Salmeron, T. Beebe, and W. Siekhaus, *J. Vac. Sci. Technol. A* **8**, 297 (1990).
- ³⁹D. F. Ogletree, R. Q. Hwang, D. M. Zeglinski, A. Lopez Vazquez-de-Parga, G. A. Somorjai, and M. Salmeron, *J. Vac. Sci. Technol. B* **9**, 886 (1991).
- ⁴⁰J. G. Forbes, A. J. Gellman, J. C. Dunphy, and M. Salmeron, *Surf. Sci.* **279**, 68 (1992).
- ⁴¹D. Bürgler, G. Tarrach, T. Schaub, R. Wiesendanger, and H.-J. Güntherodt, *Phys. Rev. B* **47**, 9963 (1993).
- ⁴²B. Marchon, P. Bernhardt, M. E. Bussell, G. A. Somorjai, M. Salmeron, and W. Siekhaus, *Phys. Rev. Lett.* **60**, 1166 (1988).
- ⁴³H. Fjellvåg, F. Grønvold, Stølen, A. F. Andresen, R. Müller-Käfer and A. Simon, *Z. Kristallogr.* **184**, 111 (1988).
- ⁴⁴I. G. Dance, *Aust. J. Chem.* **31**, 2195 (1978).

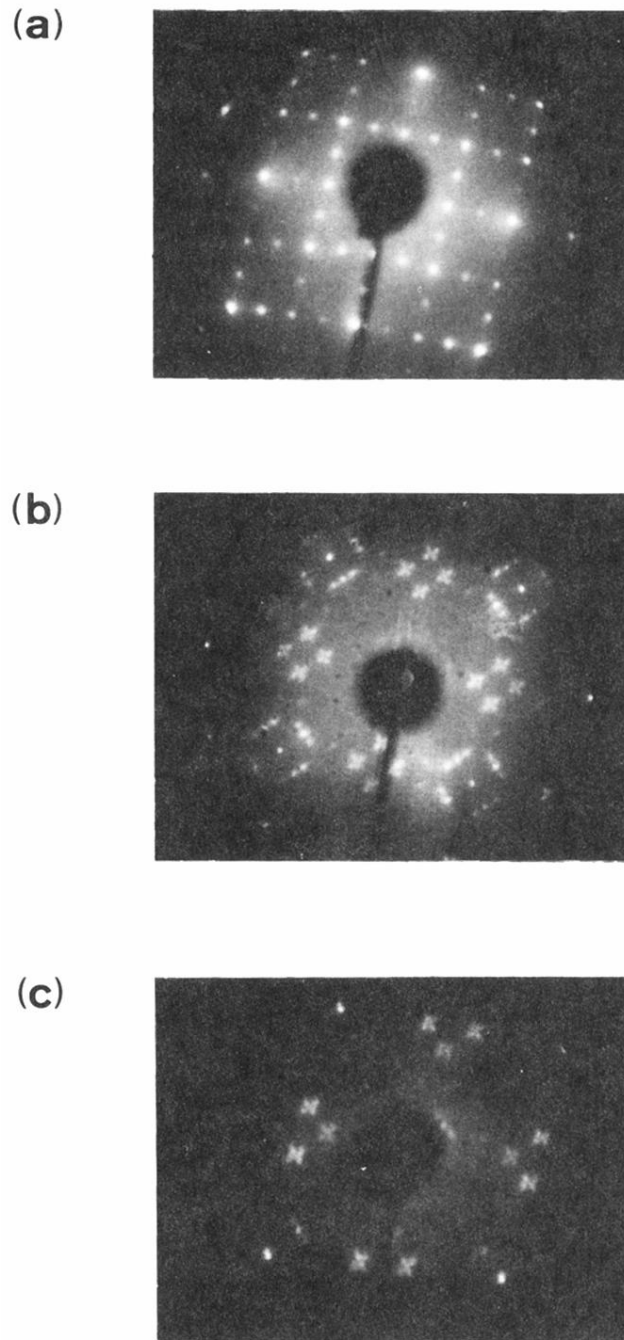


FIG. 3. LEED patterns showing O- and S-induced reconstructions of Cu(100): (a) A Cu(100)- $(2\sqrt{2} \times \sqrt{2})R45^\circ\text{-O}$ surface prepared by exposing a clean and annealed Cu(100) to 8000 L O_2 at 500 K, $E_p = 194$ eV; (b) the $|\frac{5}{2} \times \frac{3}{2}|-\text{S}$ structure formed by dosing 100 L H_2S on a Cu(100)- $(2\sqrt{2} \times \sqrt{2})R45^\circ\text{-O}$ surface at 309 K followed by annealing to 573 K, $E_p = 78.6$ eV, (c) same as (b) except $\text{H}_2\text{S} = 10$ L at 105 K, $E_p = 50.2$ eV.

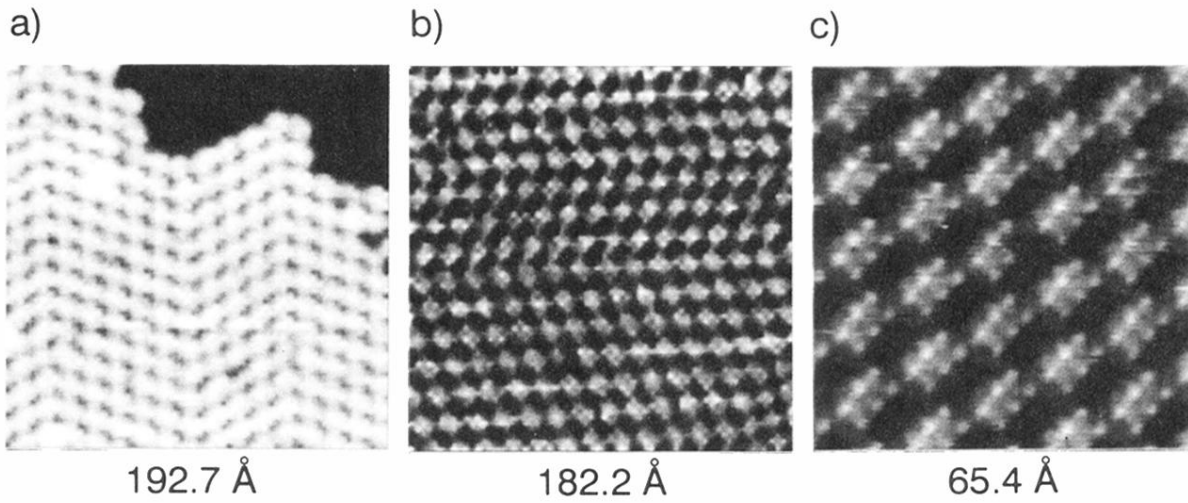


FIG. 4. STM images of the $|0 \ 2|$ -S surface prepared by dosing 100 L H_2S onto $\text{Cu}(100)-(2\sqrt{2} \times \sqrt{2})R45^\circ\text{-O}$ at 315 K followed by annealing to 573 K. All scans were performed with the sample at room temperature. Scan areas, sample bias, and tunneling currents were as follows: (a) $193 \times 193 \text{ \AA}$, $V_b = 0.65 \text{ V}$, $I_t = 1.26 \text{ nA}$, (b) $182 \times 182 \text{ \AA}$, $V_b = 0.30 \text{ V}$, $I_t = 1.06 \text{ nA}$, (c) $65 \times 65 \text{ \AA}$, $V_b = 0.64 \text{ V}$, $I_t = 1.26 \text{ nA}$.